Supporting Information

TEMPO Allegro: Liquid Catholyte Redoxmers for Nonaqueous Redox Flow

Yuyue Zhao[1,2,+], Jingjing Zhang[1,2,+], Garvit Agarwal[1,3], Zhou Yu[1,3], Rebecca E. Corman[1,4], Yilin Wang[1,4], Lily A. Robertson[1,2], Zhangxing Shi[2], Hieu Doan[1,3], Randy H. Ewoldt[1,4], Ilya A. Shkrob[1,2], Rajeev S. Assary[1,3], Lei Cheng[1,3], Venkat Srinivasan[1,5], Susan J. Babinec[5], and Lu Zhang[1,2,]*

[1] *Joint Center for Energy Storage Research, Argonne National Laboratory, Lemont, IL 60439, United States*

[2] *Chemical Sciences and Engineering Division, Argonne National Laboratory, Argonne, Illinois, 60439, United States*

[3] *Material Science Division, Argonne National Laboratory, Lemont, Illinois, 60439, United States*

[4] *Mechanical Science and Engineering, University of Illinois at Urbana−Champaign, Urbana, Illinois 61801, United States*

[5] *Argonne Collaborative Center for Energy Storage Science, Argonne National Laboratory, Lemont, IL 60439, United States*

Experimental Section:

Materials: 4-Hydroxy-2,2,6,6-tetramethylpiperidinel-oxyl (TEMPO-OH, 97%), sodium hydride (NaH, 60% dispersion in mineral oil), 2-bromoethyl methyl ether, 1-bromo-2-(2-methoxyethoxy) ethane, 1-(2-bromoethoxy)-2-(2-methoxyethoxy) ethane, lithium bis (trifluoromethanesulfonyl)imide (LiTFSI, 99.95% trace metal basis), acetonitrile (CH_3CN, electronic grade, 99.999% trace metal basis), and lithium metal (thickness of 0.75 mm) were purchased from Sigma-Aldrich. Propylene carbonate (PC), ethylene carbonate (EC), ethyl methyl carbonate (EMC), and fluoroethylene carbonate (FEC) were ordered from Gotion Co., Ltd. All the solvents and chemicals were used as received. The mixed carbonate electrolytes were dried over 3 Å molecular sieves for two days prior to use. Tosylated glycol ethers were prepared according to literature procedure. [1]

General procedure for preparation of liquid TEMPO derivatives (Scheme 1):

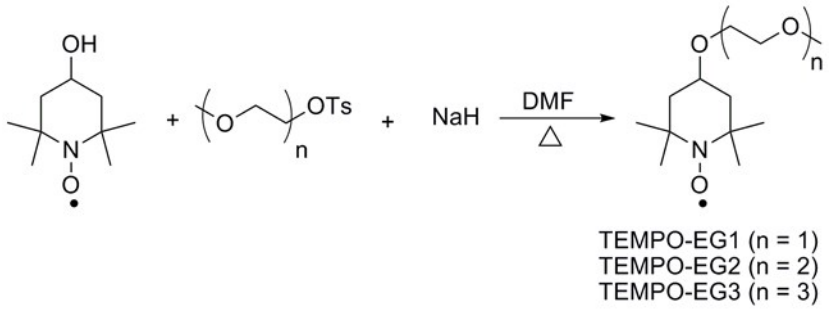

Scheme 1. Synthesis of liquid TEMPO derivatives

General synthetic procedure: 4-Hydroxy-TEMPO (5 g, 29 mmol, 1 equiv.) was dissolved in 100 mL of dry DMF, and the solution was cooled to 0 °C. NaH (60% in mineral oil, 1.2 g, 29 mmol, 1 equiv.) was added to the solution above in portions, and the reaction tempreature was maintained at < 5 °C for 30 minutes to allow complete evolution of H_2. Upon warming to the room temperature, the desired tosylated glycol ether (1 equiv.) was added, and the reaction mixture was vigorously stirred at 60 °C overnight. When the completion of the reaction was confirmed by GC-MS, the reaction mixture was cooled to room temperature, followed by addition of ice, and the solvents were removed via high vacuum distillation. The crude product was extracted into dichloromethane, washed with saturated brine (3x 10 mL), dried over $MgSO_4$, and the solvent removed in vacuo. The pure product was obtained by flash chromatography using an eluent of hexanes : dichloromethane (5 : 1, *v*/*v*) with yields of 87% (TEMPO-EG1), 84% (TEMPO-EG2), and 81% (TEMPO-EG3). The final product was characterized by GC-MS (Fig.1).

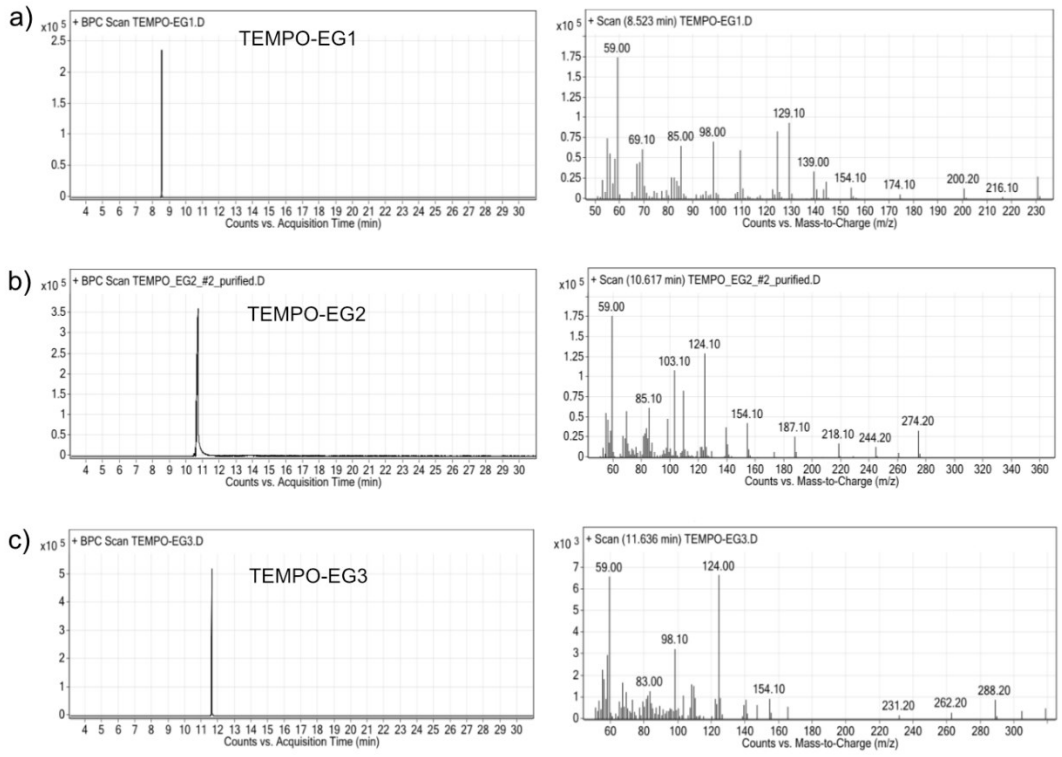

Figure S1. The GC-MS of (a) TEMPO-EG1, (b) TEMPO-EG2, (c) TEMPO-EG3

Electrochemical and kinetic measurements: Cyclic voltammograms were collected in a three-electrode configuration with iR compensation for 10 mM redoxmer solution at different sweep rates from 10 to 100 mV/s (CHI760D electrochemical workstation CH Instruments, TX). Two supporting electrolytes were used in this study, 0.5 M LiTFSI in CH_3CN and 0.5 M LiTFSI in mixed carbonate electrolytes (ethlyene carbonate:propylene carbonate:ethyl methyl carbonate or EC:PC:EMC = 4:1:5 by weight). A glassy carbon disk electrode (CHI 104, the diameter of 3 mm) and a Pt wire (CHI 115) were used as working electrode and counter electrode, respectively. A siliver/siliver nitrate ($Ag/AgNO_3$, 10 mM in CH_3CN) electrode and a Li metal were employed as the reference electrode in CH_3CN and carbonate based electrolytes, respectively.

Diffusion coefficient is an important kinetic parameter of redoxmers. Figure S2b and S4b plot of plots the anodic peak current (Ip) vs. the root of the sweep rates ($v^{1/2}$), and the resulting slopes

were then substituted into the Randles-Sevcik equation (1) to calculate the diffusion coefficient, where I_p is the anodic peak current (A); n is the number of involved electron during the electrochemical redox process; A is the effective area of the working electrode (cm^2); D stands for the diffusion coefficient of the active materials ($cm^2\ s^{-1}$); v is the sweep rate of CV measurement ($V\ s^{-1}$); c is concentration of active materials in the bulk electrolyte ($mol\ cm^{-3}$).

$$I_p = 2.69 \times 10^5\ n^{3/2}\ A\ D^{1/2}\ v^{1/2}\ c \qquad (1)$$

Galvanostatic H-cell cycling was performed in a borosilicate H-cell, which was separated by a ceramic porous membrane (P5, Adams and Chittenden) and filled with 4.0 mL of electrolyte in each half-cell. To minimize concentration polarization, the electrolyte in each chamber was stirred (~700 rpm min^{-1}). Reticulated vitreous carbon (45 PPI, ERG Aerospace Corporation) was used as working and counter electrode in the two chambers. The electrolytes containing 5 mM redoxmer and 0.5 M LiTFSI in CH_3CN were cycled between 0.1 V and 0.65 V (vs. Ag/Ag^+) for TEMPO-EG1 at a current of 5 mA. After the first cycle, the electrolyte from the counter electrode chamber was removed and replaced with fresh electrolyte as was the RVC electrode.

The hybrid flow cell was assembled by sandwiching a membrane (Daramic 800) with two pieces of carbon felt electrodes (SGL Group, SGL Technic Inc.). Prior to use, the separator and the graphite felts are dried at 80 °C for 24 h under vacuum. The effective area of the carbon felt was 2.4 cm^2 (1.5 cm × 1.6 cm). Aluminum and copper plates were employed as positive and nagative current collectors, respectively. A piece of Li metal (10 mm ×10 mm× 0.75 mm) was placed behind the graphite felt as the negative electrode, which minimizes interfacial reactions involving Li metal and thus greatly suppresses dendrite formation. A 0.1 M TEMPO-based redoxmer solution in carbonate-based electrolyte of 1 M LiTFSI (3.5 mL) was circulated using a peristaltic pump

(Masterflex L/S peristaltic pump, Cole-Parmer) at the flow rate of 20 mL min^{-1}. The cycling performance is conducted using a Neware BTS4000 (Neware Technology Limited, China) battery cycler. A range of current densities is adopted from 4 mA cm^{-2} to 12 mA cm^{-2} and the voltage cut-offs are set at 2.5 V to 4.2 V. For higher concentration cycling, an effect area of carbon felts at 9 cm^2 (3 cm × 3 cm) is used. All cycling tests are performed in a Ar filled glovebox.

Table S1. The properties of liquid TEMPO redoxmers

	TEMPO	TEMPO-EG1	TEMPO-EG2	TEMPO-EG3
Viscosity (mPa • s)	NA	10.2	10.9	21.3
Density (g cm^{-3})	~1.00	1.00	1.02	1.04
Neat concentration [a] (mol L^{-1})	NA	4.34	3.70	3.25
$E_{1/2}$ in CH_3CN electrolyte (V)	0.33	0.39	0.40	0.40
Diffusion coefficient D in CH_3CN electrolyte (10^{-6} cm^2 s^{-1})	17.3	11.90	10.20	9.78
$E_{1/2}$ in carbonate electrolyte (V)	3.54	3.59	3.60	3.60
Diffusion coefficient D in carbonate electrolyte (10^{-6} cm^2 s^{-1})	3.40	2.50	2.29	1.78

a). The concentration of neat liquid redoxmers can be calculated using the equation: $c = \frac{1000\rho}{M}$.

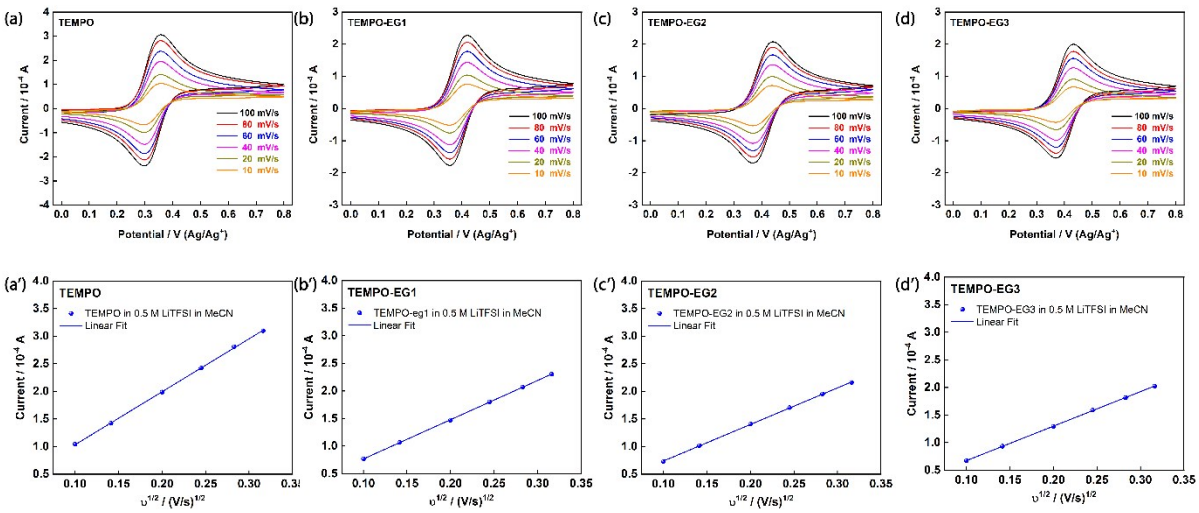

Figure S2. The cyclic voltammetry at different scan rates and the plots of I_p *vs.* (scan rate)$^{1/2}$ for TEMPO-based redoxmers: (a and a') TEMPO, (b and b') TEMPO-EG1, (c and c') TEMPO-EG2, (d and d') TEMPO-EG3 in CH_3CN-based electrolytes

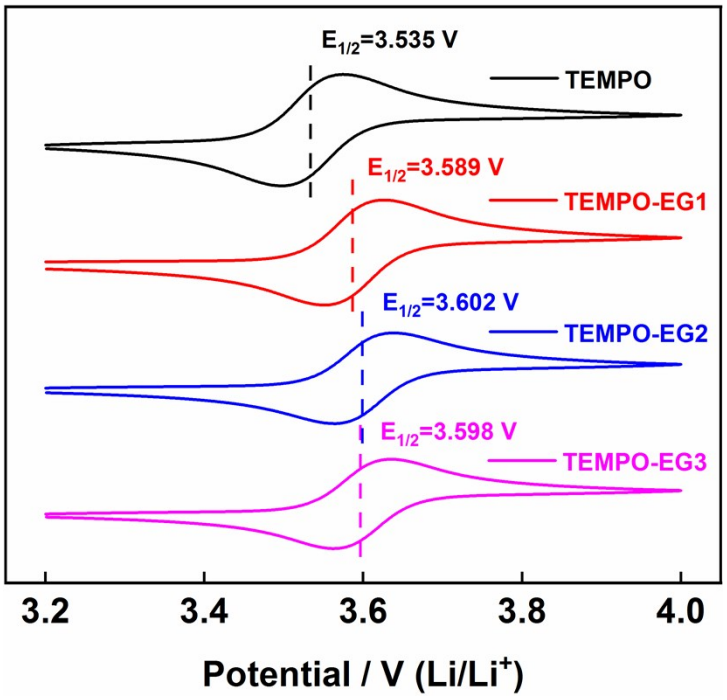

Figure S3. The cyclic voltammetry of 10 mM TEMPO-based redoxmers in a carbonate-based electrolyte (EC: PC: EMC=4:1:5 by weight) containing 0.5 M LiTFSI. Scan rate is 100 mV/s.

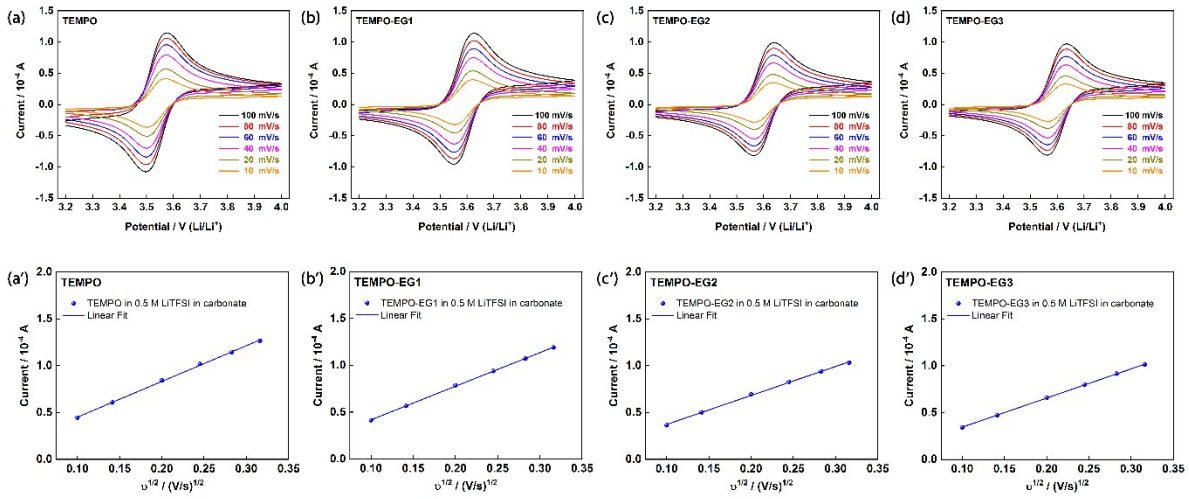

Figure S4. The cyclic voltammetry and the plots of I_p *vs.* (scan rate)$^{1/2}$ for TEMPO-based redoxmers: (a and a') TEMPO, (b and b') TEMPO-EG1, (c and c') TEMPO-EG2, (d and d') TEMPO-EG3 in a carbonate-based electrolyte (EC: PC: EMC=4:1:5 by weight) containing 0.5 M LiTFSI.

Computational Details

Oxidation Potential Calculations:

All DFT calculations were carried out using Gaussian 16 software [2] at the wb97xd/6-31+G(d,p) [3] level of theory. The geometries of the TEMPO and TEMPO-EGX molecules (TEMPO-EG1, TEMPO-EG2 and TEMPO-EG3) were optimized in the neutral and oxidized states. The free energies of solvation were computed using SMD model[4] employing CH_3CN as the solvent medium. The oxidation potentials (E^{ox} w.r.t Ag/Ag^+) were calculated using the change in Gibbs free energy (ΔG^{ox}) in solution media at 298 K upon removal of an electron from the neutral species, as given in equation 2.

$$E^{ox} = \frac{-\Delta G^{ox}}{nF} - 4.79 \text{ V} \qquad (2)$$

where F is the Faraday constant (eV) and n is the number of electrons removed from the neutral molecule (n = 1 for 1st oxidation). The constant value of '4.79 V' is subtracted to convert the

change in free energy to the reduction potential (Ag/Ag^+ reference electrode). Details regarding the computation of redox potential can be found elsewhere [5].

Diffusivity Calculations:

Classical molecular dynamics (MD) calculations were performed using GROMACS package [6] using a timestep of 2 fs. The number of Li^+, $TFSI^-$, CH_3CN, and TEMPO-EGX molecules were chosen to achieve a concentration of 10 mM for the redoxmer and 0.5 M for the LiTFSI supporting electrolyte. The non-polarizable OPLS-AA forcefield parameters were extracted from previously published work for the Li^+, $TFSI^-$ ions. [7] The forcefield parameters for the CH_3CN solvent molecules and the TEMPO-EGX redoxmer molecules were generated using LigParGen.[8] The geometries of the neutral TEMPO-EGX molecules were optimized at the B3LYP/6-311+G(d,p) level of theory and atomic partial charges for the neutral TEMPO-EGX molecules were calculated using CHELPG method using Gaussian 16.[9] The as-created system is minimized and then equilibrated using NPT ensemble for a total duration of 10 ns. The Parrinello-Rahman (PR) barostat was used to maintain a pressure of 1 atm during equilibration using NPT ensemble. [10] The temperature of the system was equilibrated at 298 K using Nose-Hoover thermostat. [10] The equilibration is followed by the final production run of 50 ns for TEMPO-EG1 molecule and 200 ns for TEMPO-EG2 and TEMPO-EG3 molecules using NVT ensemble.

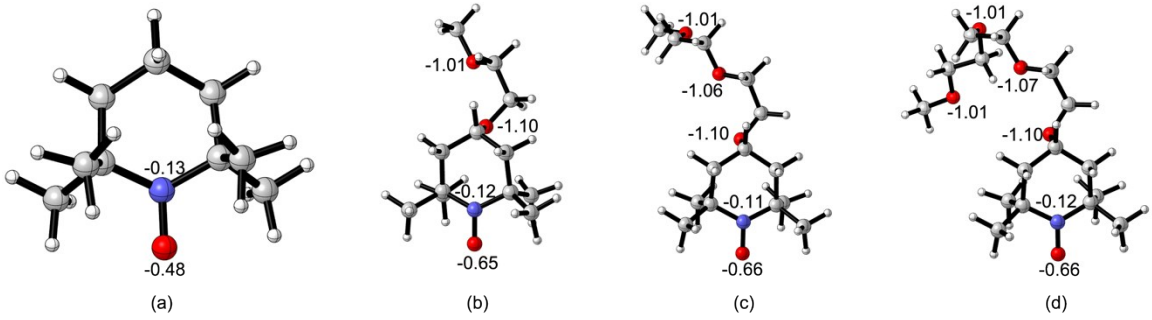

Figure S5. Computed charge distribution for (a) TEMPO, (b) TEMPO-EG1, (c) TEMPO-EG2 and (d) TEMPO-EG3 redoxmers.

Table S2: DFT computed and experimentally measured oxidation potentials (E^{ox}, vs. Ag/Ag^+, in V) for the TEMPO and TEMPO-EGX (X = 1, 2 and 3) redoxmer molecules

Molecule	Computed E^{ox} (V, Ag/Ag^+)	Experimental E^{ox} (V, Ag/Ag^+)
TEMPO	0.163	0.33
TEMPO-EG1	0.232	0.39
TEMPO-EG2	0.243	0.40
TEMPO-EG3	0.247	0.40

Table S3: MD computed and experimentally measured diffusion coefficients (D, in cm^2/s) for the TEMPO-EGX (X = 1, 2 and 3) redoxmer molecules

Molecule	Computed D x 10^{-5} (cm^2/s)	Experimental D x 10^{-5} (cm^2/s)
TEMPO-EG1	0.89	1.17
TEMPO-EG2	0.57	1.02
TEMPO-EG3	0.47	0.98

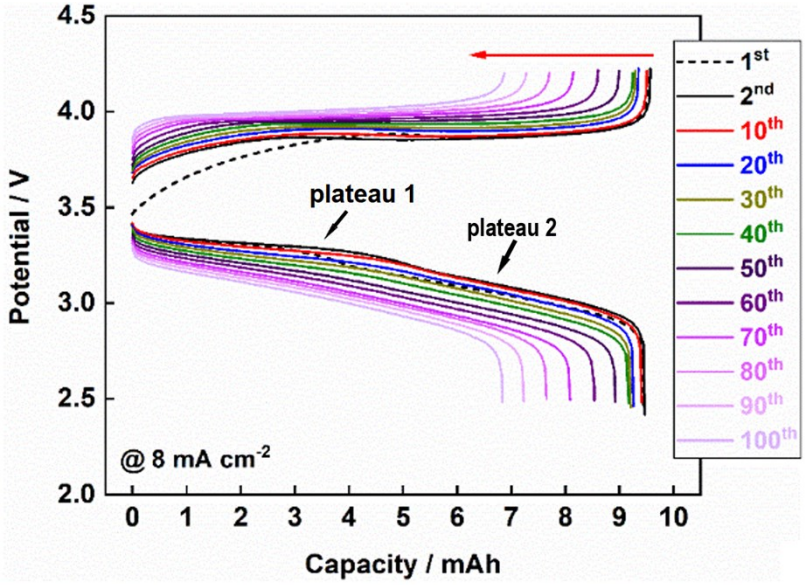

Figure S6. The voltage-capacity profiles of the hybrid flow cell containing 0.1 M TEMPO-EG1 cycled at the current density of 8 mA cm^{-2}.

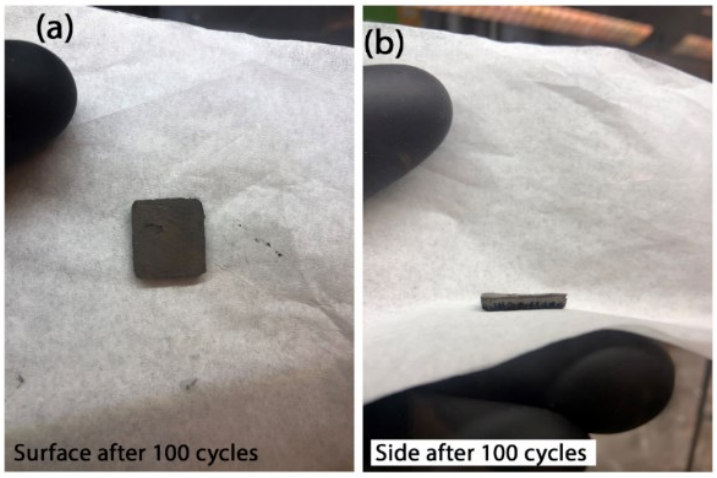

Figure S7. The images of Li deposition on the anode surface after 100 cycles: (a) the top view, (b) the side view.

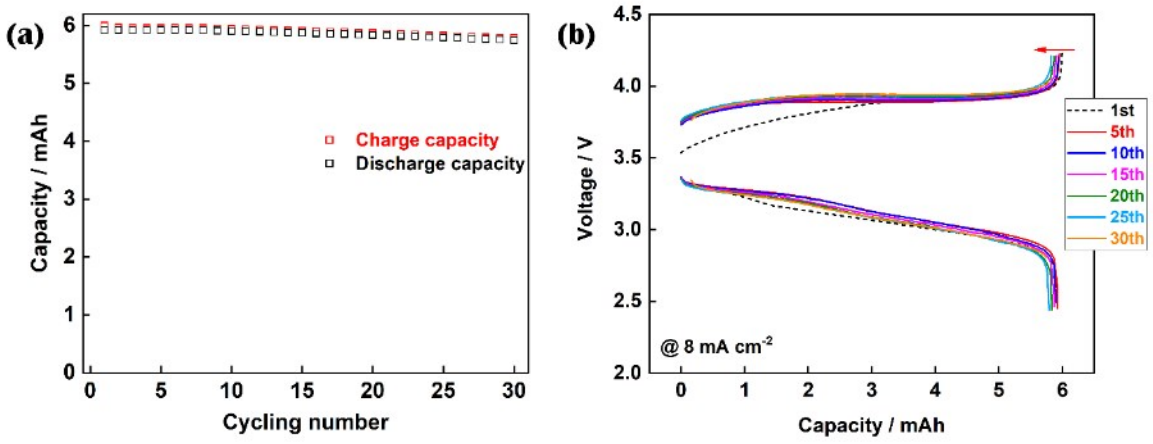

Figure S8. (a) The capacity retention (b) and voltage-capacity profiles of the hybrid cell containing 0.1 M TEMPO-EG1 after replacing the lithium-graphite anode. The current density is 8 mA/cm^2.

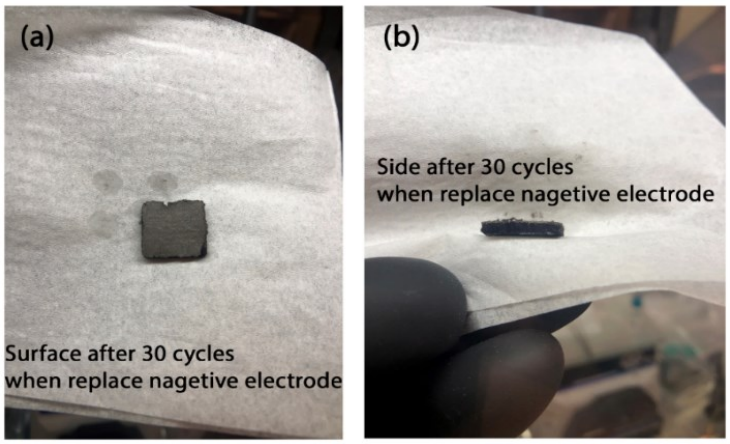

Figure S9. The images of Li deposition on the anode electrode after 30 cycles when the anode electrode was replaced: (a) the top view, (b) the side view

Table S4. Comparing performance measures of reported organic redoxmers in hybrid flow cells

Redoxmer	Potential (V v.s. Li/Li$^+$)	Concentration (mol L^{-1})	Current density (mA cm^{-2})	Energy efficiency (%)	Battery cycles	Energy density (Wh L^{-1})	Ref.
BODMA	~4.0 V	0.1	5	78	150	~10	Adv. Energy Mater. 2017, 7, 1701272
TEMPO	~ 3.5 V	0.8	5	76	30	64	Adv. Mater. 2014, 26, 7649–7653
Poly(TEMPO)	~ 3.7 V	~0.23 (repeat unit)	NA	40	NA	8.1[a]	Adv. Mater. 2016, 28, 2238–2243
TEMPO-EG1	~3.6 V	0.5	8	77	50	~21.4	this work

[a] The energy density is the theoretical energy density and others are the discharge energy density.

[1] G. W. Kabalka, M. Varma, R. S. Varma, P. C. Srivastava, F. F. Knapp, *The Journal of Organic Chemistry* **1986**, *51*, 2386-2388.

[2] M. J. Frisch, G. W. Trucks, H. B. Schlegel, G. E. Scuseria, M. A. Robb, J. R. Cheeseman, G. Scalmani, V. Barone, G. A. Petersson, H. Nakatsuji, X. Li, M. Caricato, A. V. Marenich, J. Bloino, B. G. Janesko, R. Gomperts, B. Mennucci, H. P. Hratchian, J. V. Ortiz, A. F. Izmaylov, J. L. Sonnenberg, Williams, F. Ding, F. Lipparini, F. Egidi, J. Goings, B. Peng, A. Petrone, T. Henderson, D. Ranasinghe, V. G. Zakrzewski, J. Gao, N. Rega, G. Zheng, W. Liang, M. Hada, M. Ehara, K. Toyota, R. Fukuda, J. Hasegawa, M. Ishida, T. Nakajima, Y. Honda, O. Kitao, H. Nakai, T. Vreven, K. Throssell, J. A. Montgomery Jr., J. E. Peralta, F. Ogliaro, M. J. Bearpark, J. J. Heyd, E. N. Brothers, K. N. Kudin, V. N. Staroverov, T. A. Keith, R. Kobayashi, J. Normand, K. Raghavachari, A. P. Rendell, J. C. Burant, S. S. Iyengar, J. Tomasi, M. Cossi, J. M. Millam, M. Klene, C. Adamo, R. Cammi, J. W. Ochterski, R. L. Martin, K. Morokuma, O. Farkas, J. B. Foresman, D. J. Fox, Wallingford, CT, **2016**.

[3] J.-D. Chai, M. Head-Gordon, *Physical Chemistry Chemical Physics* **2008**, *10*, 6615-6620.

[4] A. V. Marenich, C. J. Cramer, D. G. Truhlar, *The Journal of Physical Chemistry B* **2009**, *113*, 6378-6396.
[5] aJ. J. Guerard, J. S. Arey, *Journal of Chemical Theory and Computation* **2013**, *9*, 5046-5058; bJ. Moens, P. Geerlings, G. Roos, *Chemistry – A European Journal* **2007**, *13*, 8174-8184; cO. Borodin, W. Behl, T. R. Jow, *The Journal of Physical Chemistry C* **2013**, *117*, 8661-8682; dC. P. Kelly, C. J. Cramer, D. G. Truhlar, *The Journal of Physical Chemistry B* **2007**, *111*, 408-422; eG. Agarwal, H. A. Doan, R. S. Assary, *Journal of The Electrochemical Society* **2020**, *167*, 100545.
[6] B. Hess, C. Kutzner, D. van der Spoel, E. Lindahl, *Journal of Chemical Theory and Computation* **2008**, *4*, 435-447.
[7] W. L. Jorgensen, D. S. Maxwell, J. Tirado-Rives, *Journal of the American Chemical Society* **1996**, *118*, 11225-11236.
[8] aL. S. Dodda, I. Cabeza de Vaca, J. Tirado-Rives, W. L. Jorgensen, *Nucleic Acids Research* **2017**, *45*, W331-W336; bW. L. Jorgensen, J. Tirado-Rives, *Proceedings of the National Academy of Sciences of the United States of America* **2005**, *102*, 6665-6670.
[9] C. M. Breneman, K. B. Wiberg, *Journal of Computational Chemistry* **1990**, *11*, 361-373.
[10] aM. Parrinello, A. Rahman, *Journal of Applied Physics* **1981**, *52*, 7182-7190; bW. G. Hoover, *Physical Review A* **1985**, *31*, 1695-1697; cS. Nosé, M. L. Klein, *Molecular Physics* **1983**, *50*, 1055-1076; dS. Nosé, *Molecular Physics* **1984**, *52*, 255-268.